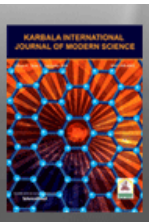

Karbala International Journal of Modern Science

Volume 6 | Issue 2 Article 4

# Influence of Carbon Fibres on Strain Sensing and Structural Properties of RC Beams without Stirrups

Arvind Kumar Cholker
*NIT Srinagar*, arvind_06phd16@nitsri.net

Manzoor Ahmad Tantray
*NIT Srinagar*, manzoor3000@yahoo.com

# Influence of Carbon Fibres on Strain Sensing and Structural Properties of RC Beams without Stirrups


## Abstract

In present study, effect of micro carbon fibres on strain sensing property and structural behavior of the reinforced concrete (RC) beams in absence of stirrups was experimentally investigated. A total of three RC beams of dimensions, 125 mm width, 350 mm height and 1500 mm long were manufactured without stirrups. All the three beams had different longitudinal reinforcement ratios (0.9%, 1.43% and 1.03 %) and uniform strength of concrete of 36.5 MPa. All the beams had carbon fibre based concrete (CFBC) at top and bottom surface in mid span for a length of 350mm and depth of 78 mm. All the beams were tested to failure under four point bending test for evaluating strain sensing property and structural behavior of carbon fibre based concrete. Fractional change in resistance (FCR) was calculated for top and bottom surface of the beam and co-related with strain in concrete and strain in tensile reinforcement. It was observed that as load increases on the beam, the FCR was increasing for the bottom surface (tension side) and decreasing for the top surface (compressive side). The trend of change in FCR for top and bottom surface is observed to be similar as that of strain in tensile reinforcement and concrete. It was also observed that, obtained FCR graphs can be used for strain and damage detection in beam. All the beams failed in shear with improved load carrying capacity as reinforcement ratio increased.



## Keywords

Strain sensing, Electrical properties, Carbon Fibers, Shear, reinforced concrete.

## 1. Introduction

Carbon fibres have attracted many researchers to work on it, as they exhibit very significant and outstanding properties such as high tensile strength, high elastic module, high fire resistance, very low electrical resistance, fracture toughness, etc,. The application of these fibres to concrete has been found to improve the mechanical properties of concrete and to increase the electrical conductivity of cement composites. Different types of carbon fibres like nano fibres [1], micro fibres, single wall carbon nano-tubes (SWNT) [2], multi wall carbon fibre [3], single carbon black [4], carbon nano tubes [5], bucky paper have been used in different studies by different researchers.

An ordinary concrete, in which short and distinct fibres are distributed uniformly, in order to improve their electrical properties is named as Carbon fibre based concrete (CFBC) here. Though many researchers have used the term fibre reinforced concrete in their work [6,7], it would be preferable to use the term as fibre based concrete. This is because; the addition of microfibres in concrete changes the matrix properties as in case of geo polymer concrete but does not improve the strength.

Good work on structural health monitoring using the above listed carbon fibres has been published from the last decade, using them either individually or in combination with other fibres. Initially, it was observed that cement based composites incorporated with carbon fibres have some electrical sensation which can be co-related to applied load [8,9]. This gave initiation for developing structural health monitoring using carbon fibres in cement and concrete composites. Later this study was extended for co-relating change in electrical resistance with compressive strain in case of cement cubes [10,11]. Further extending this work, same cement composites were used for co-relating change in resistance with deflection in case of flexural loading [12,13]. This concrete when embedded with carbon fibres is named as smart concrete/self-sensing concrete/intrinsic concrete/ self-monitoring/electrically conductive concrete.

Recent study by O. Galao et al. [14] concluded that under compressive load, CNF cement paste with 2% fibre cured for 28 days can be successfully used as a strain and damage detecting sensor. Similar study conducted on concrete cylinders by F. Azhari et al. [15] found that, under compressive loading, concrete incorporated with 15% carbon fibres can be used as strain and micro crack detecting sensor. A. Downey et al. [16] proposed resistor mesh model for detecting damage in concrete structure, constructed with conductive cement composites and also validated experimentally on cement composites containing MWCNT. Further extending this work on beams, study by Chung [17] on cement composite beam element of dimension 160 × 40 × 40 mm incorporated with carbon fibres was found to be a good indicator for strain and damage upon flexural loading. This study concluded that change in surface resistance on tension (bottom surface) side is a good indicator of damage which increases upon loading and change in surface resistance on compression surface (top surface) is a good indicator of both strain and damage sensing that decreases upon loading. Y. Ding [18] conducted study on concrete beam embedded with triphasic conductive materials, namely steel fibre, carbon fibre and nano carbon black for improving ductility and conductivity of concrete. The results concluded that, upon flexural loading, at tension side, the measured fractional change in surface impedance could be correlated linearly with crack opening displacement along with improved flexural strength and ductility of concrete. R. N. Howser [19] conducted self-sensing test on self-compacting concrete columns embedded with CNF and steel fibres. This study found that CNF fibres showed better co-relation with the applied uniaxial load. Recently, carbon fibre based concrete was also used for traffic monitoring [2] and also for de-icing of pavements as multi phase conductive admixture [20].

Therefore, from literature review it is observed that less work has been reported on RCC beams, embedded with carbon fibres that can be used for health monitoring of concrete. Hence, it is very important to study this behavior on medium scale beams and to know the probability of application of this technique on live structures for health monitoring, along with effect of carbon fibre on structural properties of conventional concrete. Therefore, this study attempts to check whether this type of health monitoring using smart concrete is applicable to medium scale RCC beams or not.

## 2. Experimental programme

### *2.1. Mixture proportions and material properties*

After performing number of trial mixes, self-compacting concrete mix having adequate performance

https://doi.org/10.33640/2405-609X.1389

was chosen for the manufacturing of RC beams. The mix should possess reasonable flow-ability in plastic state according to EFNARC [21] and desired strength in hardened state [22]. SCC was prepared using 43 grade Portland cement with specific gravity of 3.15, locally available fine aggregate and coarse aggregate having specific gravities of 2.69 and 2.74 respectively. The maximum size of coarse aggregate adopted was 10 mm and zone II fine aggregate was used for casting RC beams. Water-Cement ratio of 0.38 and high range Polycarboxylate Ether (PCE) based water reducer was also used for uniform distribution of fibres and to obtain required flow in the concrete. The constituent proportion of self-compacting concrete SCC mix adapted for the study is shown in Table 1.

Casting of all the beams was done in steel moulds and companion concrete cubes were casted in standard steel moulds of 150 mm dimension. For each beam, 3 cubes were casted to check its compressive strength. All the specimens were de-moulded after 24 h and kept for curing in the water tank for 28 days. All the beams were sunned/insolated/solarized after removing from water tank (curing) so that there is no water in the concrete and obtained electrical values are moisture free. HYSD longitudinal bars were used in present study, whose properties are shown in Table 2. Carbon Fibres (CF) of type SYC-TR-PU were added 1.5% by weight of cement in concrete mix whose properties are shown in Table 3. All the beams had uniform dimensions with length 1500 mm, width 125 mm and depth 350 mm. Since all the beams were tested for flexural performance, no shear and compression reinforcement were provided. Thus, steel bars of different diameters were provided as passive reinforcement on the tension side.

Table 1
Mix proportion for SCC.

| S. No. | Materials | Quantity/$m^3$ of concrete in kgs | Remarks |
|---|---|---|---|
| 1 | Cement | 550 | PC-43 grade with compressive strength of 43 MPa |
| 2 | Fine Aggregate | 786 | Zone-III and FM-2.56 |
| 3 | Coarse Aggregate (10 mm) | 853 | F.M-6.88 |
| 4 | Water Ready Admixture | 5.5 | PCE based super plasticizer |
| 5 | Surfactant | 0.32 | Dedocyl Benzenesulphonic acid sodium salt (SDBS) |
| 6 | Water | 209 | Tap water with pH 7.1 |
| 7 | Carbon Fibre | 7.425 | Electrically Conductive Fibres |

Table 2
Material properties of reinforcement.

| Steel type | ds (mm) | As ($mm^2$) | fy (MPa) | fu (MPa) | Es (GPa) |
|---|---|---|---|---|---|
| Longitudinal reinforcement | 12 | 113 | 690 | 771.9 | 200 |
| | 16 | 201 | 545 | 687.1 | 198 |

*ds* = diameter of steel bar; *As* = area of reinforcement; *fy* = yielding strength; *fu* = ultimate.

Table 3
Properties of carbon fibres.

| Carbon Content | % | 95 |
|---|---|---|
| Electrical Resistivity | w.cm | $1.54 \times 10^{-3}$ |
| Elongation | % | 2.3 |
| Tensile Strength | MPa | 4810 |
| Tensile Modulus | GPa | 225 |
| Density | $g/cm^3$ | 1.78 |
| Filament Diameter | μm | 6.97 |
| Length | mm | 6 |

### 2.2. Fibre based concrete

In present study, concrete embedded with carbon fibre named as carbon fibre based self-compacting concrete (CFBC) was used only in the middle portion of 350 mm length and 78 mm depth as shown in Fig. 1. CFBC is used to record the electrical resistance behavior in top and bottom layer of concrete beam in order to check strain and damage sensing property upon loading. CFBC was prepared simultaneously with the main concrete that was used for beams. The proportion of materials for carbon fibre based self compacting concrete (CFBC) was the same as used in main mix that is shown in Table 1. Carbon fibre based self-compacting concrete was prepared using 1.5% [23] of micro carbon fibres by weight of cement whose properties are shown in Table 3. For uniform distribution and to avoid lumps of fibres, firstly a solution of water required for concrete quantity and the surfactant named Dedocyl Benzene sulphonic acid sodium salt (SDBS) was prepared. Then fibres were added to this solution, and the amalgam was mechanically churned for about ten minutes. This process ensured effective and uniform distribution of fibres in the water. The other quantities of concrete mix were then blended in a mixture and the above fibre based solution was added gradually, that resulted in the production of SCC having random but uniform distribution of fibres.

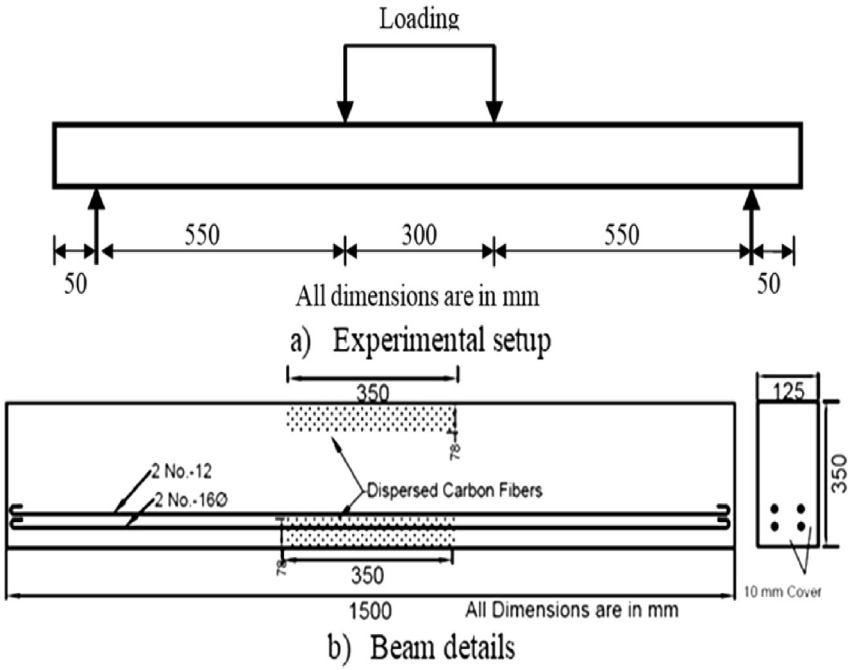


Fig. 1. a) Test setup and b) Details of tested beams.

## 3. Test setup and instrumentation

In the present study, three RCC beams were manufactured and tested under four point loading with the constant shear span in order to investigate the strain sensing and damage sensing behavior using carbon. Reinforcement and dimension details of the beam, along with test setup, are shown in Table 4 and Fig. 1 respectively. All the beams were designated using letters and numbers as shown in Table 4 for convenient reference. In beam M3-A-350, M3 represents grade of concrete, 350 represents depth and letter 'A' represents reinforcement ratio and so on.

### 3.1. Data acquisition setup

All the beams were tested to failure in order to investigate the effect of micro carbon fibres on strain, damage sensing and also to know the effect of longitudinal reinforcement on flexural performance of CFBC. Load on the beam was gradually applied using hydraulic jack of 50 ton capacity. Complete test set up is shown in Fig. 1. The applied load on beam was recorded using a load cell of 500 kN capacity and the mid span deflection, top and bottom surface strains were measured using LVDT's in the pure bending region. Strain in reinforcement was obtained using strain gauges attached to reinforcements that were embedded in concrete. During testing, load, deflections and strain readings were recorded automatically using data logger.

For measuring electrical resistance, initially electrical conductive paint was applied on top and bottom surface of RC beam just next to the point of application of the load on the inside face as shown in Fig. 2. Copper wire was adhered on top of this conductive paint using adhesive tapes to ensure that complete and continuous surface readings were obtained. The ends

Table 4
Beam properties.

| Beam Designation | Grade of concrete | b (mm) | Height D (mm) | d (mm) | Length (mm) | Ast | ρs/% |
|---|---|---|---|---|---|---|---|
| M3-A-350 | 36.2 | 125 | 350 | 340 | 1500 | 2−16Φ | 0.92 |
| M3-B-350 | 36.4 | 125 | 350 | 340 | 1500 | 2−16Φ,2−12Φ | 1.43 |
| M3-C-350 | 35.8 | 125 | 350 | 340 | 1500 | 2−12Φ,2−12Φ | 1.03 |

Note: $b$ = width of the web; $d$ = effective depth; $\rho s$ = longitudinal reinforcement ratio.

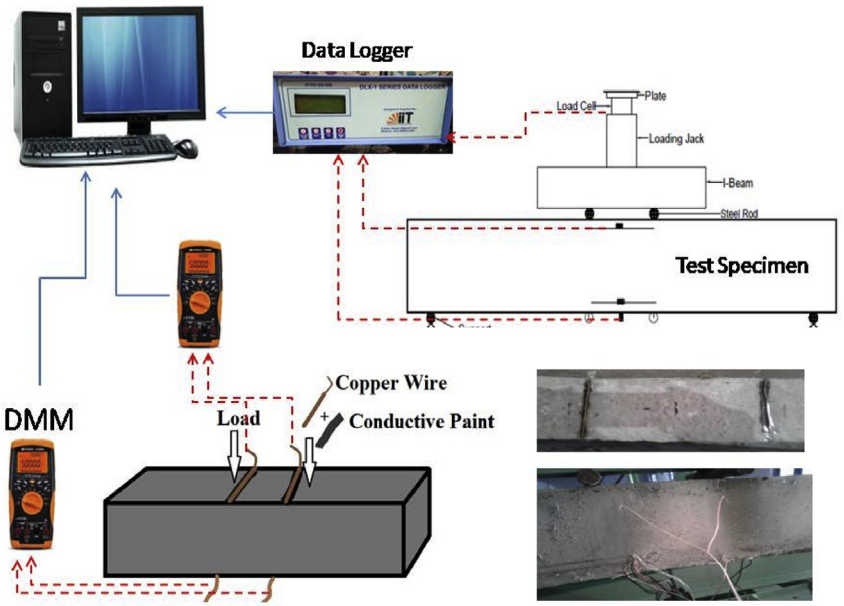


Fig. 2. Instrumentation of test setup.

of copper wires, attached to top and bottom surface of RC beam were connected to two separate digital multimeter (DMM) (Keysight U1252B) for measuring change in electrical resistance readings. Further, these DMM's and data logger were connected to the computer. The depiction of complete instrumentation is shown in Fig. 2.

## 4. Experimental results and discussions

### 4.1. SEM analysis

Concrete samples embedded with carbon fibres have been studied using SEM analysis to obtain fibre distribution in concrete. Fig. 3 shows the SEM image of fibre based concrete in amalgam and hardened state. It is observed that carbon fibres have uniformly dispersed in the concrete which is very important for making concrete as self-sensing and to obtain strain–damage sensing properties under loading. The SEM images were taken after failure of beam to see the dispersion of fibres in hardened concrete.

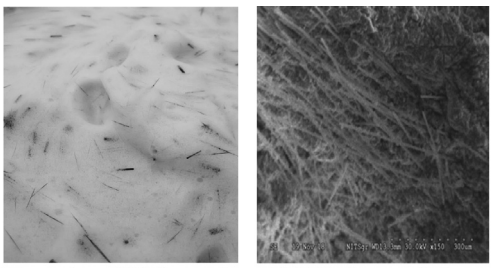

a) Dispersion of CF in amalgam b) SEM image of dispersed CF in the concrete

Fig. 3. a) Dispersion of CF in amalgam b) SEM image of dispersed CF in the concrete.

### 4.2. Electrical investigation

As discussed earlier that in order to check electrical resistance property of RC beam upon flexural loading, during casting of RCC beam, carbon fibre based self-compacting concrete (CFBC) was introduced in the mid span region for a length of 350 mm and for a depth of 78 mm at the top and bottom surface of the beam. The main objective of this work is to see the extent of co-relation between change in resistance of compression (top) and tension (bottom) surface of a RC beam during loading with that of top and bottom strains of the beam. The top strain refers to compressive strain in concrete and bottom strain refers to tensile strain in reinforcement.

#### 4.2.1. Initial resistance

Prior to load application, initial surface resistance of compression and tension side was measured using DMM. Fig. 4 shows the initial surface resistance of top and bottom surfaces. It was observed that, initial

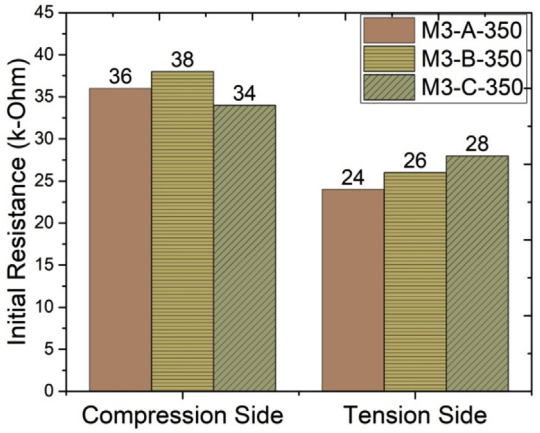


Fig. 4. Initial resistance of compression and tension surface.

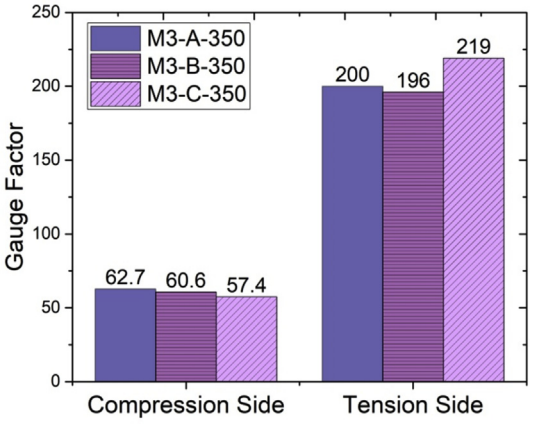


Fig. 5. GF's for of CFBC at compression and tension side.

resistance for tension side was less when compared to compression side. This is due to the fact that, presence of reinforcement in the tension side improves the conductivity in RCC beam. Studies reported that presence of reinforcement gave better co-relation of change in resistance with deflection when compared to absence of reinforcement at tension side [11]. As fibres were added to concrete, the initial resistance was observed to be in kilo-ohms that should be actually for a self-sensing concrete, as normal concrete resistance was observed to be in mega-ohms [24]. This reduction in initial resistance indicated that fibres had dispersed uniformly, and concrete obtained conductivity property, as it is very important and required for stain and damage sensing. It was also observed that the initial resistance deviation was very less indicating, fibre based concrete was uniform in all the beams.

### 4.2.2. Gauge factors of CFBC

Strain sensitivity of carbon fibre based concrete can be measured by a tool called as gauge factor (GF). This gauge factor can be defined as the fractional change in the electrical resistance per unit strain [25–27]. Fractional change in electrical resistance (FCR) and Gauge factor can be calculated using Equations (1) and (2) respectively.

$$\mathrm{FCR} = \frac{\Delta R}{R_0} = \frac{R - R_0}{R_0} \tag{1}$$

$$GF = \frac{(\Delta R|R_0)}{\Delta \epsilon} = \frac{(\Delta R|R_0)}{(\epsilon_{pc} - 0)} \tag{2}$$

where ΔR is change in electrical resistance; R0 is initial resistance; R is resistance at failure/crack loading; Δε is change strain.

The comparative gauge factor values of all the beams has been calculated using above equation and is shown in Fig. 5. From the obtained results it was observed that, GF at compression side was less compared to tension side and were ranging between 60 and 200 and are much higher than that of the commercially conventional gauge factor involving metal (approximately 2). This is probably because of presence of reinforcement that increased strain sensing sensitivity of the CFBC at tension side. Similar growth in GF's (enhanced damage-sensing property) was observed by Nguyen et al. [27], when macro-steel fibre-reinforced concrete (MSFRCs) was embedded with 0.5 vol.% micro carbon fibres.

### 4.2.3. FCR and compressive strain

During experimental testing of RC beam, load was gradually applied till failure of the beam and change in resistance during load application was recorded in the mid span, separately on compression (top) and tension (bottom) surface, using two separate DMM's. Compressive strain in concrete was measured using LVDT mounted on beam and tensile strain in reinforcement was measured using strain gauges attached to reinforcement embedded in concrete.

Fractional change in resistance (FCR) was calculated using Equation (3) from experimentally obtained electrical resistance values during testing. Both FCR and compressive strains were plotted with respect to time during load application up to failure and are shown in Fig. 6. It was observed that, as load increases, the overall strain in concrete at the top surface and

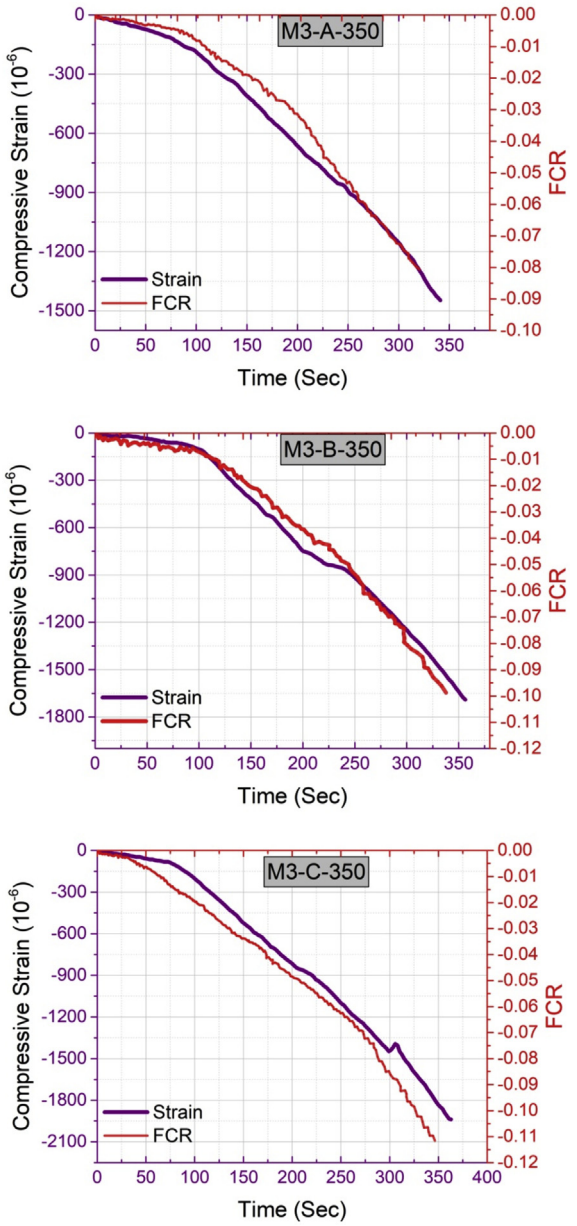


Fig. 6. Compressive strain and FCR at compression (top) surface.

FCR decreases. This trend is possible because, during the flexural test, the top surface of the beam is under compression and hence carbon fibres present in the concrete at top surface move towards each other under compression that enhances the flow of electrical charges resulting in less resistance. The similar trend was observed for all the beams regardless of variable reinforcement ratio.

$$FCR = \frac{\Delta R}{R_0} = \frac{R - R_0}{R_0} \quad (3)$$

From Fig. 6 it can be seen that the trend of decrease in concrete strain and FCR was quite comparable. As load increases on the beam, with the passage of time, curve of compressive strain of concrete decreases. During the same time period, FCR in fibre based

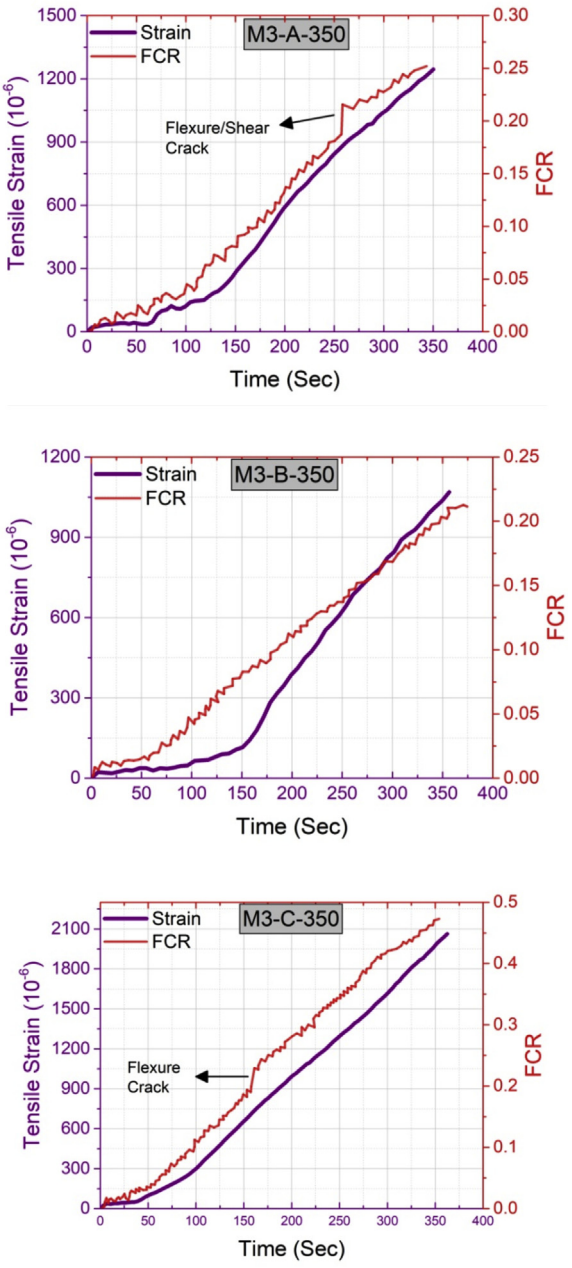


Fig. 7. Tensile strain and FCR at tension (bottom) surface.

concrete was also plotted and it was observed that both the curves follow similar trend till failure of the beam. It was also observed that, in the initial stage of 100 s, both FCR and strain in compressive concrete surface remained at low levels. Observed strains and FCR for beams M3-A, M3-B and M3-C-350 are 193 μs, 106 μs 210 μs and 0.0048, 0.0067,0.002 respectively during above said time period. This trend is probably due to the reason that, at initial loading, concrete did not compress much for the smaller loads, resulting in low strain and FCR reading. After the initial time period of 100 s, both FCR and strains were decreasing linearly up to the failure of the beam with respect to time. Negative values of both FCR and strain indicate that, as load increases, the distance between concrete surfaces under compression decreases that resulted in less resistance due to more flow of charges because of fibre movement towards each other. Maximum Fractional change in resistance for beam M3-A, M3-B and M3-C-350 are observed to be 0.08, 0.098 and 0.11 respectively.

### 4.2.4. FCR and tensile strain

Plot of tensile stain in reinforcement and FCR at the tension surface of the beam is shown in Fig. 7. It was observed that as loading increases with passage of time, FCR of tension surface and strain in reinforcement remained at low levels for the initial time period of 50 s and there after both were increasing simultaneously and linearly up to failure of the beam. It is important to note that, the variation of FCR was uniformly increasing up to the formation of micro cracks in the beam. The moment micro crack appeared at tension surface, there was sudden increase in FCR at that point with further linear increment. This variation was due to the formation of micro crack, causing discontinuity in the beam resulting in debonding and separation of fibres with each other and also with concrete, thereby reducing flow of charge and consequent increase in resistance. It was observed that, for beams M3-A-350 and M3-C-350 there was sudden increase in FCR curve at time 250 and 150 s respectively as shown in Fig. 7. This sudden increase in curve of FCR was due to the formation of micro flexural cracks that represents damage sensing property of CFBC. In case of the beam M3-B-350, there were no micro cracks in the mid-span of the beam and hence

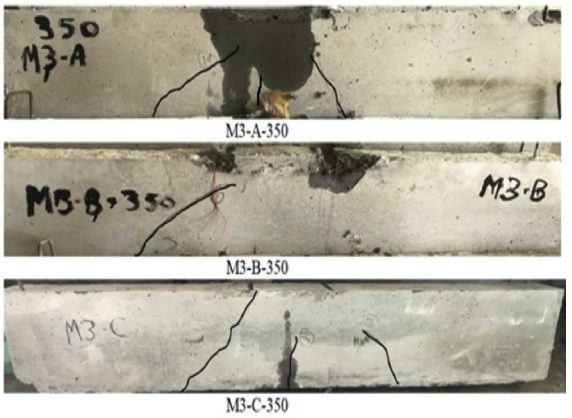


Fig. 8. Crack patterns of test beams.

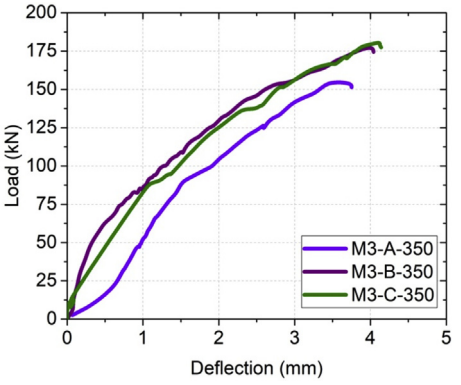


Fig. 9. Curves for mid span deflection for applied load.

Table 5
Summary of tested beams.

| Beam Designation | Ultimate state | | Initial Shear Cracking load | Exp. shear Vexp, kN | Normalized shear Vexp/ $\sqrt{f'cbd}$, Mpa | Mid-span Concrete strain at failure, μs | Mid-span Reinforcement strain at failure, μs | Failure |
|---|---|---|---|---|---|---|---|---|
| | Pu/kN | Δu/mm | Vcr/kN | | | | | |
| M3-A-350 | 151.39 | 3.75 | 120.2 | 75.695 | 0.181627 | −1446.48 | 1245 | DTF |
| M3-B-350 | 177.80 | 4.03 | 152.3 | 88.9 | 0.189504 | −1689.85 | 1150 | DTF |
| M3-C-350 | 180.82 | 4.13 | 142.5 | 90.41 | 0.199239 | −1937.68 | 2063 | DTF |

the FCR curve was increasing linearly and uniformly up to failure of the beam. Therefore, it can be said that carbon fibre based concrete can be used for strain sensing and also damage sensing purpose for RC beams. The maximum readings of FCR for beams M3-A, M3-B and M3-C are observed to be 0.25, 0.21 and 0.47 respectively.

### 4.3. Structural behavior

#### 4.3.1. Failure mode and crack pattern

The important parameters of experimental results are summarized in Table 5. The comparison of the crack pattern of beams is shown in Fig. 8. As discussed, beams M3-A and M3-C have initially cracked in flexure at the low applied load in the mid-span. As the load increased further, and reached ultimate capacity beam failed due to diagonal tension. It was observed that, no beam failed due to crushing of concrete or yielding of reinforcement but the beam M3-C-350 failed suddenly without giving warning prior to failure.

#### 4.3.2. Load versus mid-span deflection curves

Fig. 9 shows mid span deflection of all the tested beams under four-point loading with respect to the applied load. The role of different parameter on the structural behavior of tested beams is described as below.

#### 4.3.3. Longitudinal reinforcement ratio

From the graph of load deflection curves shown in Fig. 9, it is found that, reinforcement ratio has significant role on the ultimate load carrying capacity. It is observed that beam with lower reinforcement ratio (M3-A-350) showed less deflection before failure compared to other beams. As the percentage of reinforcement ratio increased, the ultimate deflection also increased. In beam M3-B-350, that had highest reinforcement ratio showed same deflection as that of M3-C-350. Therefore, it can be said that, beam deflection is the main function of beam depth. As there was no shear reinforcement provided, beams could not resist shear cracking and failed due to diagonal tension failure. Due to this reason, though all the beams had different reinforcement ratios, load carrying capacities and ultimate deflections of all the beams were more or less same. Since all the beams failed in diagonal tension failure, there was no yielding of reinforcement or it can be said that beams failed prior to yielding of reinforcement resulting in very less deflection. The ultimate loads carried by beams M3-A, M3-B and M3-C are 151.39 kN, 177.80 kN and 180.82 kN with a maximum deflection of 3.75 mm, 4.03 mm and 4.13 mm respectively.

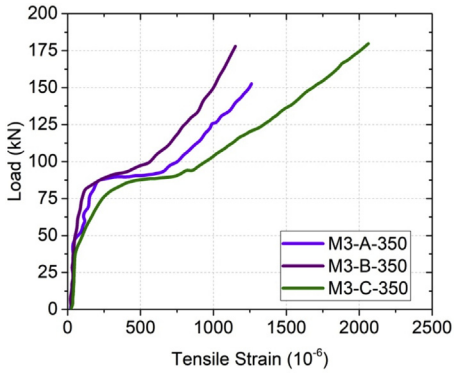


Fig. 10. Load versus reinforcement strain of mid span section.

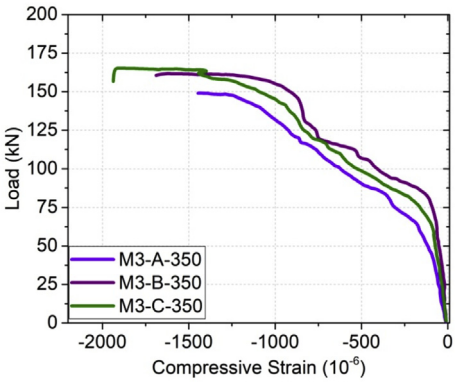


Fig. 11. Load versus concrete strain of mid span section.

#### 4.3.4. Load versus top and bottom concrete surface strains

The plot of tensile strain in flexural reinforcement and top surface strain of concrete under compression of all the beams at the mid span section with respect to applied load is shown in Figs. 10 and 11 respectively. Positive values of strain refer to tension in reinforcement while the negative refer to compression in the top concrete surface.

In all the beams, as the reinforcement ratio increased, both compressive and tensile strain was observed to be increasing. For all the beams, both tensile strain in reinforcement and compressive strain in concrete remained at low levels for small loads of 75 kN. As load increased beyond 75 kN, there was sudden increase in reinforcement strain from 250μs to 750 μs for a small amount of increase in load, from 85 kN to 100 kN. As load increased beyond 100 kN, strain in steel was increasing linearly that continued up to failure of the beam. In case

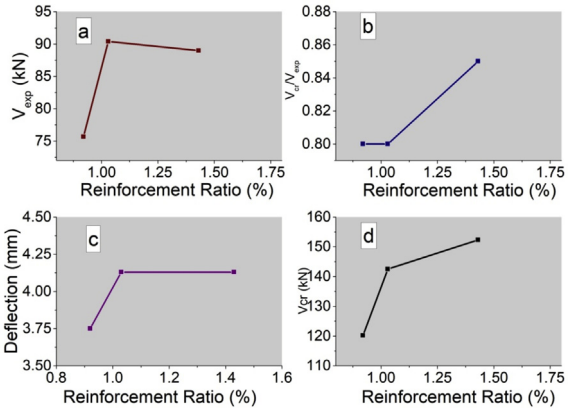


Fig. 12. a) Reinforcement ratio and Ultimate shear failure load b) Reinforcement ratio and Vcr/ Vexp c) Reinforcement ratio and deflection d) Reinforcement ratio and Initial shear cracking load.

of the beam M3-C-350, that had two bars of same diameter showed more strain at same load levels compared to other beams having different diameter bars. Beam M3-B-350 having 2−16 mm and 2−12 mm diameter bars with maximum reinforcement ratio showed less strain compared to other beams. From Fig. 10 it was observed that, in none of the beams reinforcement yielding was observed and hence it can be said that failure of the beam was not due to yielding of reinforcement. From Fig. 11 it was observed that compressive strain in concrete was also remained at low levels for initial loading up to 75 kN and there after it showed nonlinear increase. It was observed that in all the beams, though load carrying capacity was different, strain in concrete was more or less same with a maximum value of 1800 μs. This indicates that, in no beam concrete reached ultimate strain and failure was due to diagonal tension failure only rather than compression of concrete.

### *4.3.5. Effect of flexural reinforcement ratio on shear strength*

From previous studies, it was observed that on shear strength, both the elastic modulus and flexural reinforcement have nearly same effect and effect of these two parameters gives axial stiffness when combined ρf Ef. Therefore, in present study, only the effect of reinforcement ratio is investigated having constant elastic modulus. Fig. 12(a), (b), (c) and (d) shows the plot of experimental shear force, ratio of cracking shear to ultimate experimental shear force, deflection and cracking shear force respectively against variable reinforcement ratio.

It was observed that as the reinforcement ratio increases from 0.92% to 1.03% keeping all other parameters of the beam as constant, ultimate shear force increases by 15% but further increase in reinforcement ratio from 1.03% to 1.43%, the same strength has reduced by 1.5% as shown in Fig. 12(a). This is probably due to the reason that, addition reinforcement beyond 1.03% increased beam stiffness making beam rigid. In Fig. 12(c) it is observed that with increasing in reinforcement ratio, initial shear cracking capacity of the beam increased by 15.6% for 1.03% reinforcement ratio and 21% for 1.43% reinforcement ratio when compared with 0.92% reinforcement ratio. It is worth to note from Fig. 12(b) that, beams with reinforcement ratio of 0.93% and 1.03% had nearly same Vcr/Vexp value of 0.78 and 0.79. This is because, being reinforcement ratio difference very small, the ratio of cracking shear to ultimate shear was same though the initial shear cracking load and ultimate shear forces were different. Beam that had reinforcement ratio of 1.43% showed a maximum Vcr/Vexp value of 0.85.

### *4.3.6. Strut and tie model*

To check the effect of carbon fibres, obtained experimental values of shear stress have been compared with strut and tie model and are shown in Table 6. Equations (4)−(6) have been used for calculating shear stresses using strut and tie model that can be found in any basic text book of reinforced concrete structures [28,29]. From Table 6 it can be said that experimental and theoretical values are quite

Table 6
Experimental and strut and tie (model) shear stress comparison.

| S.No. | Beam Designation | Beam Properties | | Concrete compressive Strength (MPa) | Shear Strength (MPa) and their comparison | | |
|---|---|---|---|---|---|---|---|
| | | | | | Expt. | Strut and Tie | $V_{S\&T}/V_{exp}$ |
| | | ρ/% | a/d | | $V_{exp}$ | $V_{S\&T}$ | |
| 1 | M3-A-350 | 0.92 | 1.62 | 36.2 | 1.8 | 2.10 | 1.24 |
| 2 | M3-B-350 | 1.43 | 1.62 | 36.4 | 2.09 | 2.26 | 1.08 |
| 3 | M3-C-350 | 1.02 | 1.62 | 35.8 | 2.13 | 2.21 | 1.04 |

Vexp - Experimental Shear stress; VS&T − Shear stress using strut and tie model (theoretical).

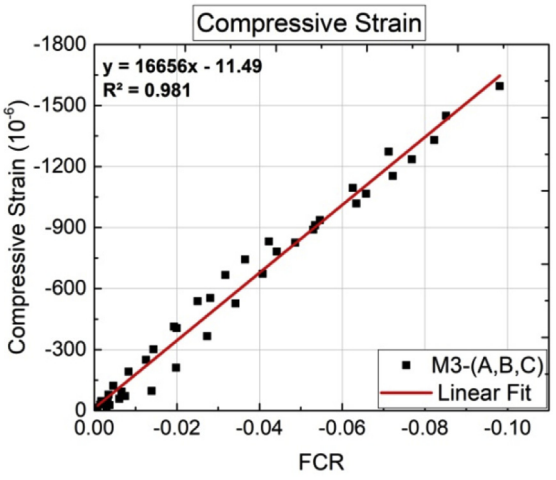


Fig. 13. Relationship between FCR and compressive strain.

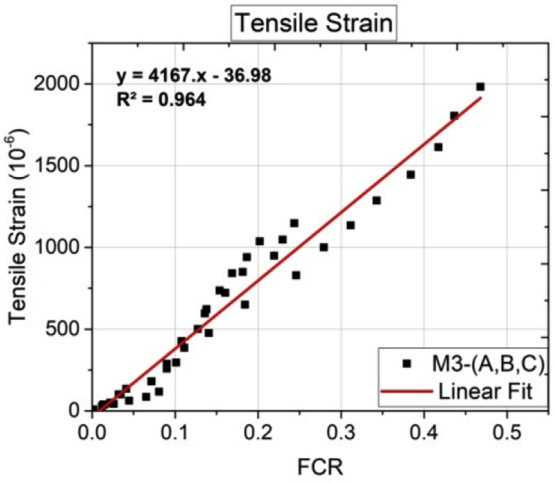


Fig. 14. Relationship between FCR and tensile strain.

comparable, thus concluding that presence of fibres does not affect the strength of the beam much.

$$P_U \leq \eta f_c^{'} b w_c \ \ldots \tag{4}$$

$$\eta = 1.25 - \frac{f_c^{'}}{500} - 0.72\left(\frac{a}{d}\right) + 0.18\left(\frac{a}{d}\right)^2 \leq 0.85 \ldots \quad for\ a/d < 2 \ \ldots \tag{5}$$

$$w_c = \frac{f_y A_{st}}{\eta f_c^{'} b} \ \ldots \tag{6}$$

Table 7
Fitted parameters of regression equation.

| Strain Type | Constant b | Constant a | Correlation coefficient R2 |
|---|---|---|---|
| Compressive strain | 16,656 | −11.49 | 0.98 |
| Tensile strain | 5167 | −36.98 | 0.96 |

where $P_U$ is ultimate load, $f_c^{'}$ is concrete compressive strength, $b$ is width of the beam, a is shear span and d is depth of the beam.

### 4.4. Influence of carbon fibres on relationship between FCR and strains

Fig. 13 and Fig. 14 shows the scatter plot of compressive strain and tensile strain with respect to FCR values for all the beams that is obtained by nominalization the curves shown in Figs. 7 and 8 respectively with respect to time.

Using regression analysis, it was observed that, there was monotone relation between compressive/tensile and FCR at compressive and tension side with linear correlation between Strain and FCR. The relation between compressive/tensile strain (represented by Y) and FCR (represented by X) can be expressed as

$$\boldsymbol{Y = b.X + a} \tag{7}$$

Where **b** and **a** are constantan parameters denoting **b** as the slope of fitting line and **a** as the intercept. The values of **a** and **b** for compressive and tensile strains are tabulated in Table 7 along with correlation coefficients with values. The correlation coefficients ($\mathbf{R^2}$) values in both the graphs show the good correlation between FCR and compressive/tensile strains. Using Equation (7) strain (compressive/tensile) at any point can be obtained if FCR is known. This helps in continues monitoring of a beam as a NDT (non destructive test) approach, if resistance is measured using carbon fibres that are incorporated in beam.

## 5. Conclusions

An experimental study on electrical and structural performance on carbon fibre based concrete RC beams without stirrups under four points loading was conducted to investigate the strain, damage sensing behaviour and effect of fibre based concrete on RC beams with variable reinforcement ratios. Based on the experimental results following conclusions were drawn:

- From electrical investigation it was found that, concrete embedded with carbon fibres in proper proportion, can be used for strain sensing purpose as it gains strain sensing property due to presence of conductive fibres as admixture.
- It was observed that, variation of fractional change in resistance (FCR) at compression side and tension side was similar with that of compressive strain in concrete and tensile strain in reinforcement respectively. It was also observed that variation in reinforcement ratio did not affect the electrical properties of CFBC.
- From obtained equations, correlating strain and FCR, compressive/tensile strain can be obtained at any point/time, if FCR is known. This gives an NDT approach for measuring strains in beam at any point of loading giving a new approach of continues structural health monitoring.
- In structural properties, it is observed that, flexural reinforcement ratio significantly affect the behavior and shear strength of the beam. With the increase in reinforcement ratio both shear strength and stiffness are observed to be enhancing.
- Beam that had reinforcement ratio of 1.43 failed abruptly without giving any failure warning due to increase in brittleness of the beam because of presence of high reinforcement ratio compared to M3-A beam that had lower reinforcement.
- Obtained experimental values of shear stress, when compared with the theoretical model (strut and tie model) showed that, addition of carbon fibres to concrete does not affect strength significantly, as fibres being micro in diameter did not bridge the cracks because of extremely low bond strength i.e., borne by the circumference of the fibre.

## References


[1] J. Hoheneder, I. Flores-Vivian, Z. Lin, P. Zilberman, K. Sobolev, The performance of stress-sensing smart fibre reinforced composites in moist and sodium chloride environments, Compos. B Eng. 73 (2015) 89–95, https://doi.org/10.1016/j.compositesb.2014.12.028.

[2] B. Han, X. Yu, E. Kwon, A self-sensing carbon nanotube/cement composite for traffic monitoring, Nanotechnology 44 (2009) 445501, https://doi.org/10.1088/0957-4484/20/44/445501.

[3] H.K. Kim, I.W. Nam, H.K. Lee, Enhanced effect of carbon nanotube on mechanical and electrical properties of cement composites by incorporation of silica fume, Compos. Struct. 107 (2014) 60–69, https://doi.org/10.1016/j.compstruct.2013.07.042.

[4] L. Shi, Y. Lu, Y. Bai, Mechanical and Electrical Characterisation of Steel Fibre and Carbon Black Engineered Cementitious Composites, vol. 188, 2017, pp. 325–332, https://doi.org/10.1016/j.proeng.2017.04.491.

[5] M. Sánchez, M. Campo, A. Jiménez-Suárez, A. Ureña, Effect of the carbon nanotube functionalization on flexural properties of multiscale carbon fibre/epoxy composites manufactured by VARIM, Compos. B Eng. 45 (1) (2013) 1613–1619, https://doi.org/10.1016/j.compositesb.2012.09.063.

[6] V. Kodur, R. Solhmirzaei, A. Agrawal, E.M. Aziz, P. Soroushian, Analysis of fl exural and shear resistance of ultra high performance fi ber reinforced concrete beams without stirrups, Eng. Struct. 174 (2018) 873–884, https://doi.org/10.1016/j.engstruct.2018.08.010.

[7] F.J. Baeza, O. Galao, E. Zornoza, P. Garcés, Effect of aspect ratio on strain sensing capacity of carbon fibre reinforced cement composites, Mater. Des. 51 (2013) 1085–1094, https://doi.org/10.1016/j.matdes.2013.05.010.

[8] S. Wen, D.D.L. Chung, Piezoresistivity-based strain sensing in carbon fibre-reinforced cement, ACI Mater. J. 104 (2) (2007) 171.

[9] H. Chen, C. Qian, C. Liang, W. Kang, An approach for predicting the compressive strength of cement-based materials exposed to sulfate attack, PloS One 13 (2018) 1–11, https://doi.org/10.1371/journal.pone.0191370.

[10] S. Wen, D.D.L. Chung, Strain-sensing characteristics of carbon fibre-reinforced cement, ACI Mater. J. 102 (4) (2005) 244.

[11] B. Han, K. Zhang, X. Yu, E. Kwon, J. Ou, Electrical characteristics and pressure-sensitive response measurements of carboxyl MWNT/cement composites, Cement Concr. Compos. 34 (2012) 794–800, https://doi.org/10.1016/j.cemconcomp.2012.02.012.

[12] S. Wen, D.D.L. Chung, Strain-sensing characteristics of carbon fibre.pdf, ACI Mater. J. 102 (2005) 244–247.

[13] X. Fu, D.D.L. Chung, Effect of curing age on the self-monitoring behavior of carbon fibre reinforced mortar, Cement Concr. Res. 27 (9) (1997) 1313–1318, https://doi.org/10.1016/S0008-8846(97)00118-X.

[14] O. Galao, F.J. Baeza, E. Zornoza, P. Garcés, Strain and damage sensing properties on multifunctional cement composites with CNF admixture, Cement Concr. Compos. 46 (2014) 90–98, https://doi.org/10.1016/j.cemconcomp.2013.11.009.

[15] F. Azhari, N. Banthia, Cement & Concrete Composites Cement-based sensors with carbon fibres and carbon nanotubes for piezoresistive sensing 34 (2012) 866–873.

[16] A. Downey, A. D'Alessandro, M. Baquera, E. García-Macías, D. Rolfes, F. Ubertini, S. Laflamme, R. Castro-Triguero, Damage detection, localization and quantification in conductive smart concrete structures using a resistor mesh model, Eng. Struct. 148 (2017) 924–935, https://doi.org/10.1016/j.engstruct.2017.07.022.

[17] S. Wen, D.D.L. Chung, Self-sensing of flexural damage and strain in carbon fibre reinforced cement and effect of embedded steel reinforcing bars, Carbon N. Y. 44 (8) (2006) 1496–1502, https://doi.org/10.1016/j.carbon.2005.12.009.

[18] Y. Ding, Z. Han, Y. Zhang, J.B. Aguiar, Concrete with triphasic conductive materials for self-monitoring of cracking development subjected to flexure, Compos. Struct. 138 (2016) 184–191, https://doi.org/10.1016/j.compstruct.2015.11.051.

[19] R.N. Howser, H.B. Dhonde, Y.L. Mo, Self-sensing of carbon nanofibre concrete columns subjected to reversed cyclic loading, Smart Mater. Struct. 20 (8) (2011), 085031, https://doi.org/10.1088/0964-1726/20/8/085031.

[20] J. Wu, J. Liu, F. Yang, Three-phase composite conductive concrete for pavement deicing, Construct. Build. Mater. 75 (2015) 129–135, https://doi.org/10.1016/j.conbuildmat.2014.11.004.

[21] EFNARC, Specification, Guidelines for self-compacting concrete, 32, Association House, London, UK, 2002, p. 34.
[22] ACI Committee 237, 237R-7 Self-Consolidating Concrete, MI, USA, 2007.
[23] A.K. Cholker, M.A. Tantray, Mechanical and Durability Properties of Self-Compacting Concrete Reinforced with Carbon Fibres, 2019, pp. 1738−1743.
[24] A. D'Alessandro, M. Rallini, F. Ubertini, A.L. Materazzi, J.M. Kenny, Investigations on scalable fabrication procedures for self-sensing carbon nanotube cement-matrix composites for SHM applications, Cement Concr. Compos. 65 (2016) 200−213, https://doi.org/10.1016/j.cemconcomp.2015.11.001.
[25] D.L. Nguyen, J. Song, C. Manathamsombat, D.J. Kim, Composites : Part B Comparative electromechanical damage-sensing behaviors of six strain-hardening steel fibre-reinforced cementitious composites under direct tension, Compos. PART B. 69 (2015) 159−168, https://doi.org/10.1016/j.compositesb.2014.09.037.
[26] A.K. Cholker, M.A. Tantray, Strain-sensing characteristics of self-consolidating concrete with micro-carbon fibre, Aust. J. Civ. Eng. (2019) 1−10, https://doi.org/10.1080/14488353.2019.1704206.
[27] D. Nguyen, D. Kim, D. Thai, Concrete by adding low amount of discrete carbons, Materials 12 (6) (2019) 938, https://doi.org/10.3390/ma12060938.
[28] K.S. Ismail, M. Guadagnini, K. Pilakoutas, Strut-and-Tie modeling of reinforced concrete deep beams, J. Struct. Eng. 144 (2) (2018), 04017216, https://doi.org/10.1061/(asce)st.1943-541x.0001974.
[29] Menon Devadas, Reinforced Concrete Design, Tata McGraw-Hill Education, 2003.